Int. J. Electrochem. Sci., 2 (**2007**) 947 - 957

International Journal of ELECTROCHEMICAL SCIENCE
www.electrochemsci.org

Corrosion Performance of a Rapidly Solidified NiAl Intermetallic Macroallolled with Fe in 0.5M H_2SO_4

J. Colín[1], S. Serna[2], B. Campillo[1], O. Florez[3] and J.G. González-Rodriguez[2]*

[1]UAEM-Facultad de Ciencias QUimicas e Ingeniería, AV. Universidad 1001, Col. Chamilpa. 62209-Cuernavaca, Mor., Mexico
[2]Universidad Autónoma del Estado de Morelos, CIICAp, Av. Universidad 1001, Col. Chamilpa, 62209-Cuernavaca, Mor, México
[3]Universidad Nacional Autonoma de Mexico, Instituto de Ciencias Fisicas, AV. Universidad S/N
[*]E-mail: ggonzalez@uaem.mx

Received: 28 August 2007 / *Accepted:* 19 September 2007 / *Online published:* 20 October 2007

The effect of Fe contents on the corrosion resistance of NiAl intermetallic rapidly solidified in 0.5 M H_2SO_4 at room temperature has been evaluated using electrochemical techniques. Iron contents included 15, 18 and 20 wt.% and techniques included potentiodynamic polarization curves, linear polarization resistance and potentiostatic tests. For comparison, the same tests were performed on a 316L type stainless steels. The results showed that all the intermetallics, except the alloy containing 18 Fe, exhibited a better corrosion resistance than the 316L type stainless steel for at least five times. Additions of Fe to the NiAl alloy always increased the corrosion current density, $I_{corr.}$ except by adding 20 Fe, which decreased the I_{cor} value only for long times. The pitting potential, E_{pit}, passivation potential, E_{pass} and passive current density values were higher for all the NiAL intermetallics than those values for the 316 stainless steel. Additions of Fe to the NiAl alloy always decreased these values with. Corrosion morphologies showed a preferential dissolution of a phase respect to another due to the formation of micro galvanic cells due to the addition of Fe.

Keywords: Macroalloying, aluminides, corrosion

1. INTRODUCTION

Nickel aluminide, NiAl, is an intermetallic compound that is formed as a result of the ordering of nickel and aluminum atoms on the f.c.c. unit cell. As a promising intermetallic, it can be used in both low and high temperature due to its high melting point, low density, and excellent thermal conductivity. These characteristics make nickel aluminide a promising candidate as a structural material for both ambient and high temperature applications. Although the interest of nickel

aluminides is primarily due to its potential for high temperatures applications, it also possesses certain properties which make it a good candidate for low temperature applications. NiAl corrosion resistance is due to the ability to form a dense, adherent, protective aluminum oxide, Al_2O_3, layer. However, NiAl is too brittle at room temperature and it has poor creep properties with respect to more conventional alloys [1-4]. Major efforts have been centered on enhancing its mechanical properties through grain refinement, micro and macro-alloying as well as ductile phase toughening [5-7]. Ternary additions to NiAl have been investigated by several researchers [8-10], and it has been reported, for instance, that Fe additions substitute equally for both Ni and Al. During solidification of Ni-Al alloys with ternary additions of Fe, Co, Cr or Cu, ternary elements were distributed into γ phase; in particular, Fe additions induced formation of γ phase[11], and small amounts of Fe destabilized the β phase and inducing the β martensite transformation. The aqueous, low temperature corrosion resistance of NiAl is of concern for high temperature applications because these materials will not always be operating at high temperatures but also al low temperatures, and corrosion damage during fabrication or maintenance could lead to catastrophic failures during service. Thus, the goal of this work is to investigate the effect of macroalloying a NiAl alloy with Fe in its low temperature corrosion performance.

2. EXPERIMENTAL PART

Three intermetallic alloys were induction melted in vacuum according the compositions listed in Table 1 at 1700°C and then cast it. The location of the alloys in the phase diagram is shown in Figure 1. Alloy ingots were re-melted and rapidly solidified by the melt-spinning rapid solidification technique, in which ribbons more than 10 cm length and ~100 □m thick were obtained. Wheel speed and injection pressure were ~1.5 m/s and ~14 g/mm^2 respectively and the solidification rate 10^4 K.s^{-1}.

Table 1. Localization index (LI) for tested materials

Material	**LI**
316SS	0,358557922
NiAl	0,1216122
NiAl15Fe	0,882693
NiAl18Fe	0,986660
NiAl20Fe	0,99654898

Afterwards, ribbons were cut into segments of 1 cm length and mounted in epoxy resin. To perform the corrosion test experiments, these ribbons were polished with diamond paste to a 0.1 μm finish. Electrochemical experiments were performed using an ACM Instruments potentiostat controlled by a personal computer. Potentiodynamic polarization curves (PC) were obtained by varying the applied potential from –300 mV with respect to the free corrosion potential, E_{corr}, up to +600 mV at a rate of 1mV/s. Before the experiments, the E_{corr} value was measured for approximately 30 minutes, until it was stable. All potentials were measured using a Saturated Calomel Electrode (SCE) as reference electrode. The counter electrode was a platinum wire. Corrosion rates were calculated in terms of the

corrosion current, I_{corr}, by using linear polarization resistance curves, LPR This operation was performed by polarizing the specimen from +10 to -10 mV, with respect to E_{corr}, at a scan rate of 1 mV/s (this value being a standard scanning rate for this kind of experiments) to get the polarization resistance, R_p. Using the Stearn-Geary[11] equation, the I_{corr} value was calculated as follows:

$$I_{corr} = \frac{b_a b_c}{2.3(b_a + b_c)} \bullet \frac{1}{R_P}$$

were b_a and b_c are the anodic and cathodic slopes obtained from the polarization curves. The corrosion rates, in mm/year, were calculated using Faraday´s law. All tests were performed at room temperature (25°C ± 2°C). The aqueous solutions used included 0.5M Sulfuric acid, H_2SO_4, which was prepared from analytical grade reagents. After the experiments, the specimens were cleaned to be observed in the scanning electronic microscope (SEM) and microchemical analysis of the corroded specimens were analyzed using energy dispersive spectroscopy (EDS). To see the pitting stability tendency, the current density between two identical electrodes at the free corrosion potential, E_{corr}, For comparison, all the tests were performed on a 316 type stainless steel also.

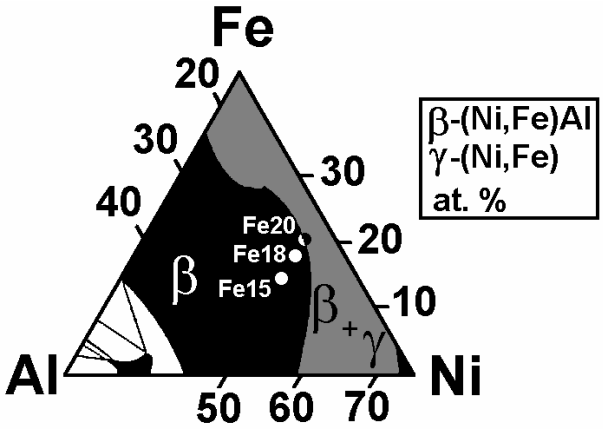

Figure 1. Ternary phase diagram of the Ni-Al-Fe system. Black points indicate the location of the alloys under study.

3. RESULTS AND DISCUSSION

3.1. Microstructural characterization

The location of the alloys in the phase diagram is shown in Fig. 1. From this figure we can see that the three alloys are within the biphasic field of the β-(Ni,Fe)Al and γ-$(Ni,Fe)_3Al$ phases. The resulting microstructure after the melt spinning process of the three alloys are given in Fig. 2. The microstructure of the NiAl-base alloy had an equiaxial dendritic microstructure formed by the β-(Ni,Al) phase, with not secondary phases or precipitates (Fig. 2a). Some pores can be observed inside the dendritic phases. For the alloys containing Fe, it can be seen that they consisted basically of an equiaxial dendritic microstructure formed by the β-(Ni,Fe)Al phase, with a slight presence of the cubic

γ-(Ni,Fe) phase as a second phase at the grain boundaries. This is expected since the location of the 15 Fe alloy is the nearest to the monophasic field of such a phase.. It is important to note that the 18Fe-containing alloy had a dendritic structure with a smaller grain size due maybe to the fact that, for this case, the solidification rate was faster than that for the 15 Fe and 20 Fe alloys.

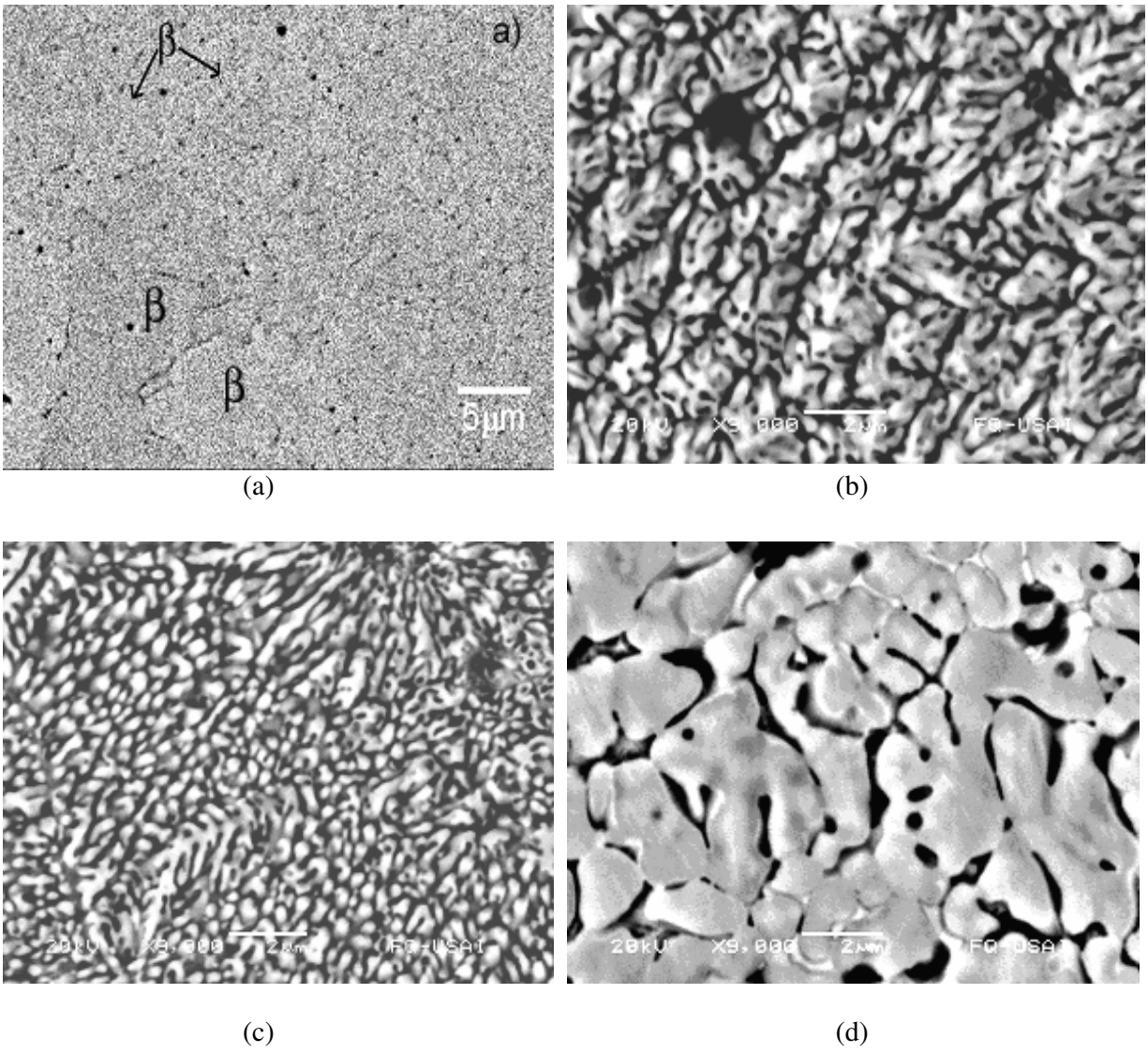

Figure 2. Microstructures of as-received NiAl alloys showing in a) NiAl, b) NiAl+15Fe, c) NiAl+18Fe and d) NiAl+20Fe specimens

3.2. Corrosion tests

Polarization curves of the different materials tested are shown in Fig. 3. The E_{corr} value of all the NiAl intermetallic alloys, except the NiAl base alloy, were more noble than the value exhibited by the 316 type stainless steel. The E_{corr} value for the unalloyed NiAl intermetallic was around 0.0 V and it was decreasing as the Fe contents increased obtaining the most active value close to –0-5 V for the

alloy with 20 Fe. All the alloys exhibited a passive behaviour also, and the pitting potential, E_{pit}, was highest for the base NiAl alloy, but additions of Fe decreased this value by nearly 0.5 V remaining constant regardless the contents of this element. The pitting potential for the 316 type stainless steel was al least 0.5 V less noble than that for the intermetallic alloys. Finally, the passive current density value was highest for the NiAl base alloy, followed by the NiAl+18Fe, whereas the lowest value was exhibited by the NiAl+15 alloy, very similar to the shown by the 316 type stainless steel.

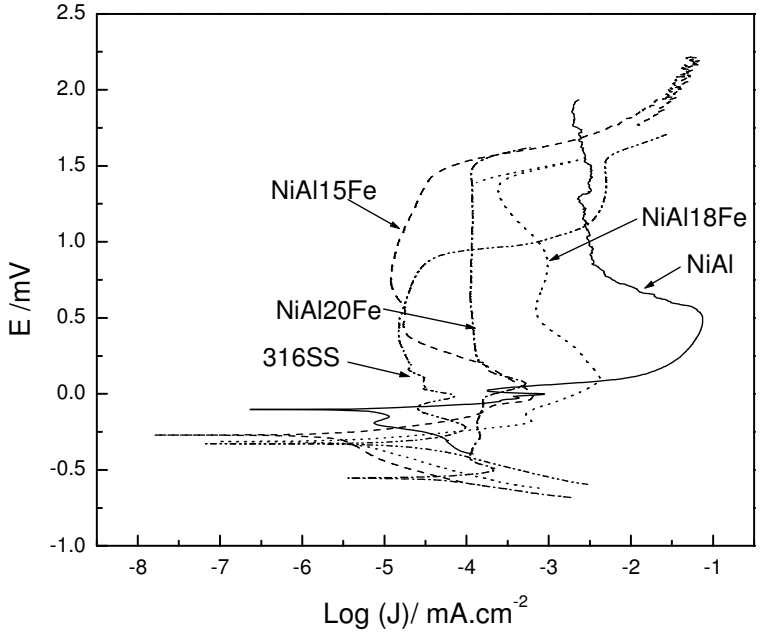

Figure 3. Effect of Fe contents on the polarization curves of NiAl intermatallic alloys.

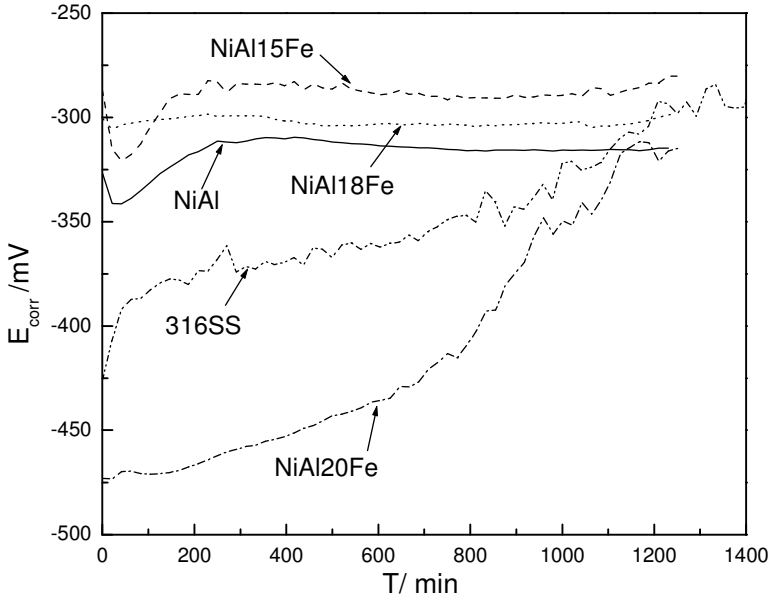

Figure 4. Effect of Fe contents on the change in the E_{corr} value with time for NiAl intermatallic alloys.

The change of the E_{corr} value with time for the different alloys is given in Fig. 4. We can see that additions of Fe to the NiAl alloy made the E_{corr} value of the NiAl to move towards less negative values for up to 100 mV, except the alloy containing 20 Fe, which had an E_{corr} more negative than the base alloy for nearly 100 mV. All the potential values of the intermetallics remained quite constant as time elapsed, which means than the passive film was very stable. The alloy containing 20 Fe had a different behaviour, which became less negative with time, and, towards the end of the test, all the alloys, even the 316 type stainless steel, had E_{corr} values very close to each other. At the same time, the E_{corr} value of the unalloyed NiAl intermetallic was less negative than the value for the 316 type stainless steel for nearly 100 mV, except the alloy containing 20Fe, which had an E_{corr} value 75 mV more negative.

On the other hand, the effect of the addition of Fe to the NiAl alloy on the corrosion current density values, I_{corr}, is shown in Fig. 5. where it can be seen that practically all the NiAl alloys had I_{corr} values lower than that for the 316 type stainless steel for at least five times, except the alloy very containing 18Fe, which had the highest I_{corr} value, up to two orders of magnitude than the base NiAl alloy. The I_{corr} value of the 316 type stainless steel was always higher than the values obtained for the NiAl alloys, but lower than that for the 18Fe containing alloy, for almost one order of magnitude.

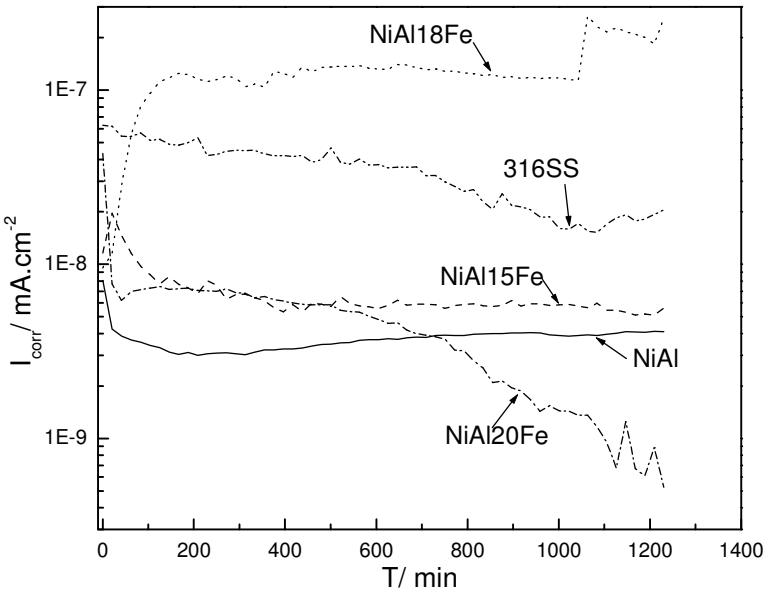

Figure 5. Effect of Fe contents on the change in the I_{corr} value with time for NiAl intermatallic alloys.

The current fluctuations of the corrosion current density for the 316 type stainless steel if given in Fig. 6. These readings, like all the current fluctuations readings for the NiAl intermetallics, were taken after a few minutes of immersion. Fig. 6 shows anodic and cathodic going transients of high intensity and high frequency. The intensity, however, decreases with time in a slow fashion. These anodic transients have been related with some kind of localized attack like pitting, preferential corrosion, stress corrosion cracking, etc…[12-14] Thus, the slow decrease in the anodic corrosion

current transients must be related with the passivation of the 316 stainless steel surface, as evidenced in its polarization curve shown in Fig. 3.

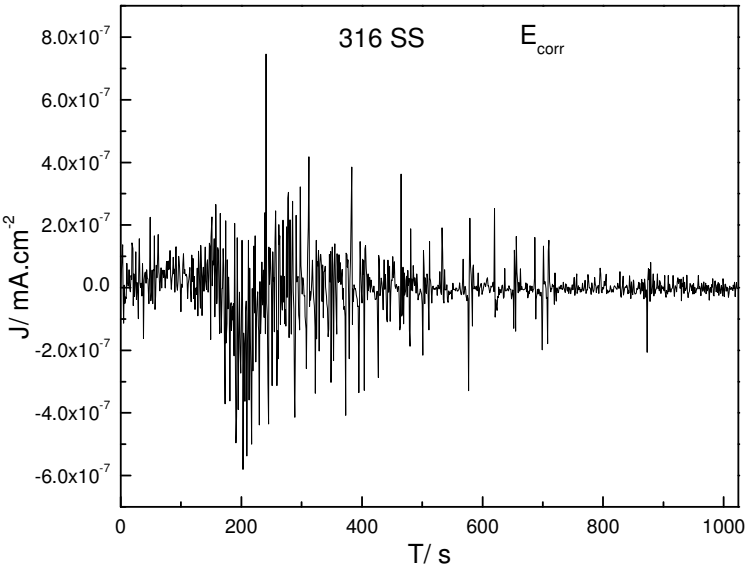

Figure 6. Current fluctuations for 316 type stainless steel at under freely corrosion conditions.

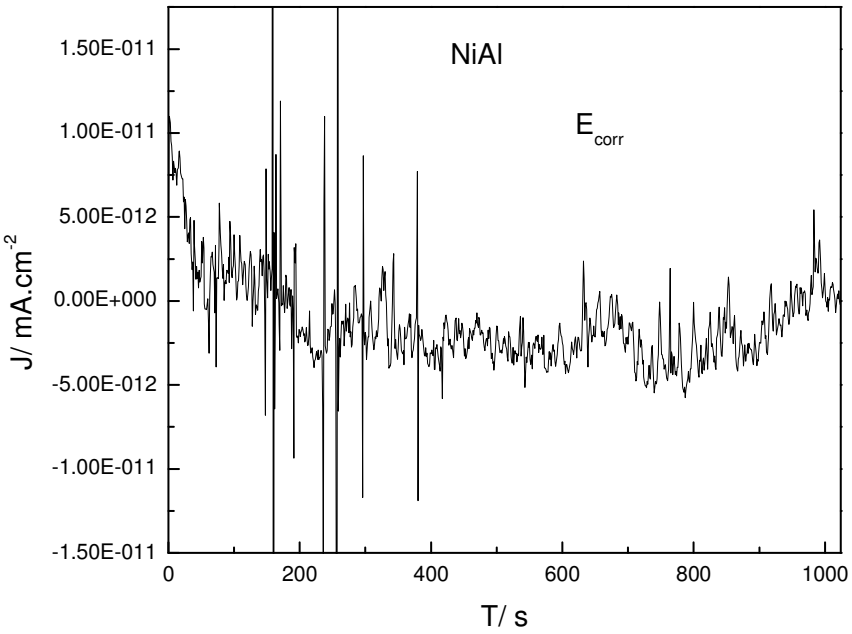

Figure 7. Current fluctuations for NiAl alloy at under freely corrosion conditions.

The unalloyed NiAl base alloy also exhibited some anodic and cathodic going transients in the corrosion current values with lower intensity than the ones exhibited by the 316 stainless steel, almost 4 orders of magnitude lower, and this intensity also decreases with time, like the 316 stainless steel,. Fig. 7. When 15 Fe was added to the NiAl alloy, the intensity of the transients with both low and high

intensity decreased, as shown on Fig. 8. where it is evident the decrease in the corrosion current density values with time. When the amount of Fe was increased up to 18%, the transients decreased in

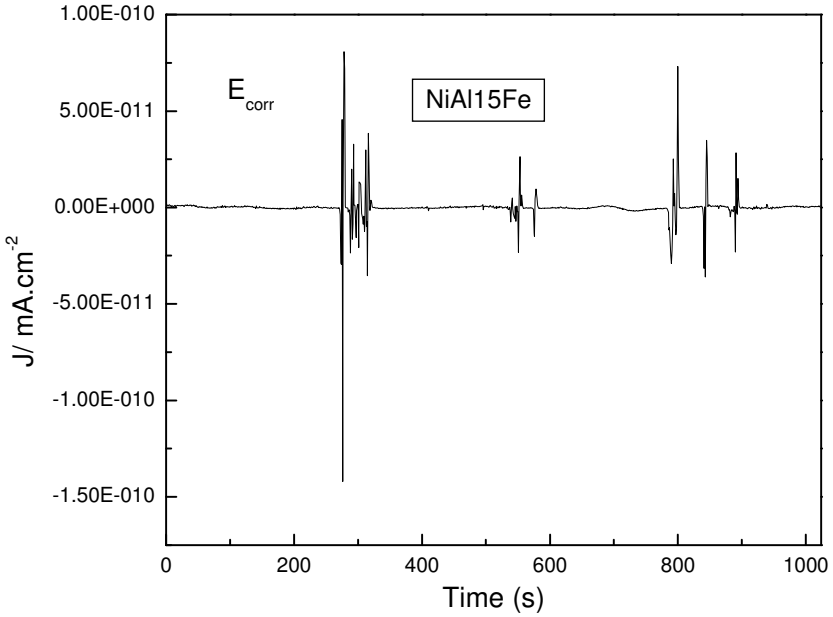

Figure 8. Current fluctuations for NiA+15Fe alloy at under freely corrosion conditions.

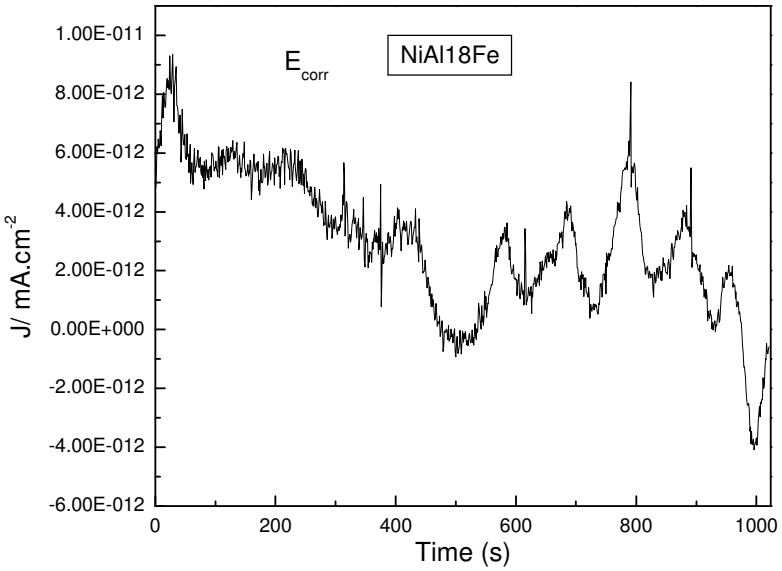

Figure 9. Current fluctuations for NiA+18Fe alloy at under freely corrosion conditions.

intensity and the transients with higher intensity but lower frequency tended to disappear, Fig. 9. The alloy containing 20Fe, however, showed the combination of transients of low and high intensity and high frequency. The transients, however, were only anodic, unlike the other intermetallics, which exhibited both. anodic and cathodic going transients, Fig. 10, with an intensity remaining constant as time elapsed, indicating that the metal surface is in a passive state[15] but undergoing localized type of

corrosion. According to the form of the intensity and frequency, this kind of behaviour has been related to a uniform, general kind of corrosion or at the best, a mixture of localized and uniform type of corrosion [14]. LI values for the different alloys under study are given in table 1. This table shows that, according to [14] all the alloys should suffer from a localized type of corrosion. However, this means that the a uniform kind of corrosion does not occur at the same time, since if some parts suffer from localized form of corrosion, in some other parts a uniform kind of corrosion is taking place.

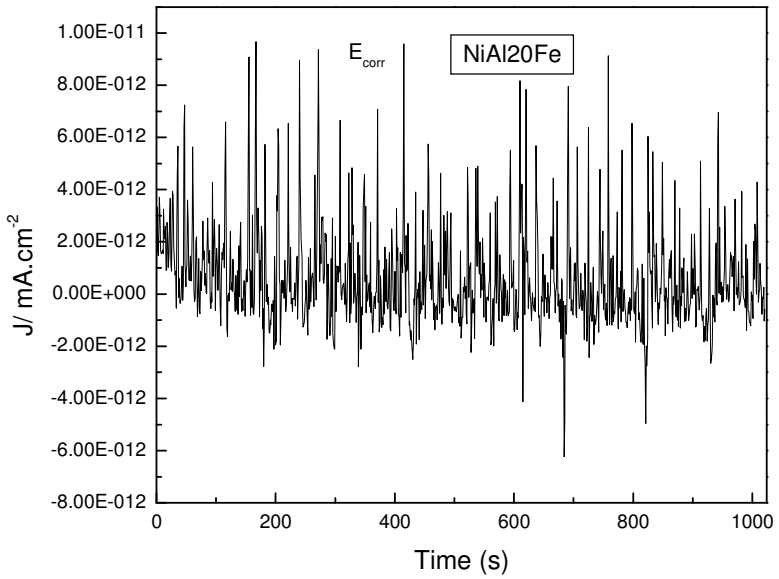

Figure 10. Current fluctuations for NiA+20Fe alloy at under freely corrosion conditions.

Surface specimens after being corroded in 0.5M H_2SO_4 are shown in Fig. 11. The unalloyed NiAl specimen did not show a uniform attack, only localized, interdendritic grain boundaries attack as shown on Fig. 11a.. However, for the 15 and 18Fe containing alloys, the β-(Ni,Fe)Al phases exhibited the localized type of attack remaining the γ-(Ni,Fe) phase unattached. For the 20Fe containing alloy, again, the β-(Ni,Fe)Al phase, i.e. the grain boundary, suffered from localized type of corrosion.

For passivation to occur, the film must be adherent, without porous, chemically inert in the solution, etc. It has been stated that, if the formed film on the alloy is flaws-free, the underlying alloy will not suffer severe corrosion, or will not be pitted, but if the film contains flaws or any other discontinuities, the alloy will suffer from corrosion. Pitting occurs as the dissolution of the metal at flaws and defects within the surface film when the bare metal is exposed to the aggressive anions in the electrolyte. The sites of pitting or localized corrosion are related to the conditions of the metal surface, such as microstructure, surface preparation, and to the composition of the electrolyte. To cause pitting, anions such as Cl^-, SO_4^-, Br^-, I^-, etc. must first adsorb on the surface of films. With anions present, pitting occurs in competition with the repair process of the passive film by the active dissolution of the metal at flaws. The presence of second phases or the establishment of micro cells, where one of the phases has either different chemical composition or microstructure, one of these phases will act as cathode and the other as an active anode. This will cause the preferential dissolution

of one of the phases, the one which acts as active anode, inducing preferential, localized dissolution within the alloy. To improve the pitting behavior, the film must avoid the adsorption of anions and delay the breakdown of passivity. The alloys containing Al are protected against corrosion by the formation of a protective Al_2O_3, alumina layer. Thus, another effect of Fe is the presence of second phases within the alloy, inducing the establishment of micro galvanic cells, and, thus, the preferential dissolution of one of the phases, the one with less corrosion resistance, which will act as active anode.

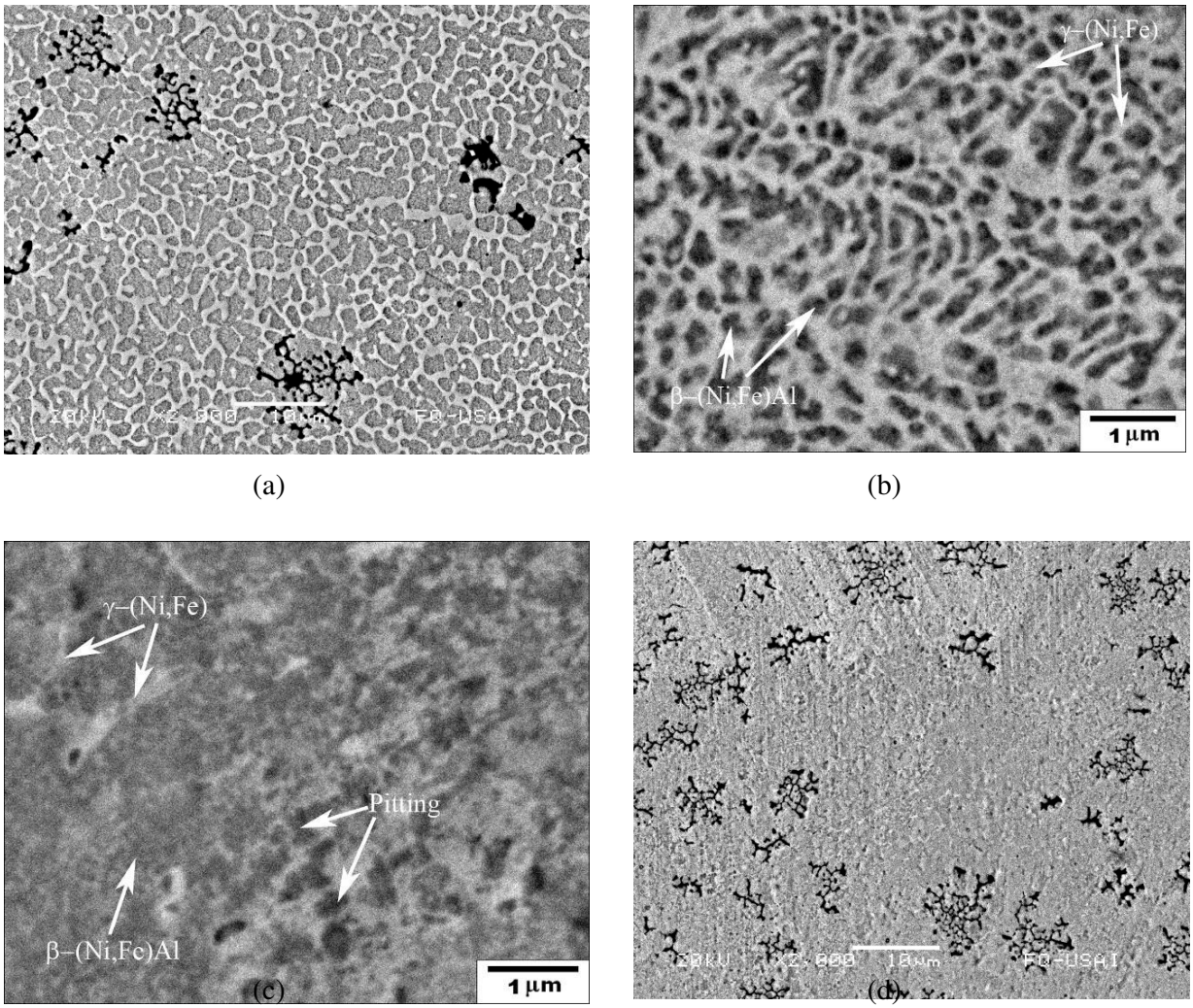

Figure 11. Micrograph of the corroded surfaces of a) NiAL, b) NiAl+15Fe, c)NiAl+18Fe and d) NiAl+20Fe alloy.

4. CONCLUSIONS

The corrosion resistance of rapidly solidified, macroalloyed with 15, 18 and 20 Fe the NiAl alloy in 0.5 M H_2SO_4 has been studied and compared with the corrosion resistance of 316 type stainless steel. The main findings are:

1. The E_{corr} values of the NiAl intermetallic alloys was always less active than the E_{corr} value obtained for 316 type stainless steel except for the alloy containing 20Fe. Additions of Fe made the E_{corr} values of the unalloyed NiAl more noble except for the alloy containing 20Fe..
2. The corrosion current density values, I_{corr}, were at least five times lower for the NiAl-xFe intermetallic alloys than of 316 stainless steel except for alloy containing 18Fe. Additions of 15, 18 and 20Fe to the base NiAl intermatallic alloy increased its I_{corr} value more than ten times. However, for long times, additions of 20Fe decreased the I_{corr} values for long times.
3. All the NiAl intermetallic alloys had higher passivation potential, E_{pass}, and pitting potential, E_{pit} than the 316 type stainless steel. In all cases, additions of Fe to the NiAl intermetallic decreased the E_{pit} value. Compared with the unalloyed NiAl alloy, additions of Fe up to 20% decreased the passive current density, I_{pass}. The lowest I_{pass} value was obtained with 15Fe, whereas the highest values was obtained with 18Fe.
4. The NiAl intermetallic alloys exhibited a preferential, localized, kind of corrosion, which was caused by the establishment of micro galvanic cells, which resulted by the formation of second phases within the alloy.

ACKNOWLEDGMENTS
to Gabriel Lara (G. Lara), L. Baños, Anselmo González and Ernesto Sánchez Colín, for their technical support.

References

1. R.D., Noebe R.R. Bowman, M.V Nathal, *Int. Mater. Rev*. 38(1993)193
2. D.B. Miracle, *Acta Metallurgica Mater*. 41(1993)649
3. R. Darolia, *J. Mater. Sci. Technol*. 10(1993)157
4. E.P. George, M.Yamagochi, K.S.Kumar, C.T.Liu, *Annu. Rev. Mater. Sci*. 24(1994)409
5. R.R.Bowman, A.K.Misra, S.M. Arnold, *Metall. Trans*. 26A(1995)615
6. H.P.Chiu,. L.M Yang, R.A Amato, *Mater. Sci. Eng A* 203(1995) 81
7. C.T Liu, L.M.Yang, R.A.Amato, *Mater. Sci. Eng A* 191(1995) 49
8. D.B.Miracle, R Darolia. in *Intermetallic Compounds: Principles and Practice*, Vol.2, J.H. Estbrook and R.L. Fleisher, ed. John Whiley and Sons, New York, (1995)53
9. G.R.Bozzolo, D., Noebe and F.Honey, *J. Intermetall* 8(2000)7
10. N.J. Medvedeva, Y.N.Gornostyrev, D.L.Novikov, O.N Myrasov. and A.J.Freeman, *Acta Metall. Mater* 46(1998)3433
11. M. Stearn and A.L. Geary, *J. Electrochem Soc*. 105(1958) 638
12. K.Hdlaky, J.L.Dawson, *Corr Sci*. 22(1982)231
13. R.A.Cottis, C.A Loto, *Corrosion* 46(1990) 12
14. J.Stewart, D.B.Wells, P.M.Scott, D.E.Williams, *Corr. Sci*.33(1992) 39
15. J.Uruchurtu-Chavarin, J.L.Dawson, *Corrosion* 47(1991)472